

**TEXTURAL AND CONCENTRATION PATTERN OF HEAVY MINERALS IN  
RED SEDIMENTS OF BADLANDS TOPOGRAPHY BHIMUNIPATNAM,  
VISAKHAPATNAM DIST., INDIA**

**T. Laxmi<sup>\*</sup>, P. Nishad<sup>\*\*</sup>, K.E. Jayadevan<sup>\*\*</sup> and R. Bhima Rao<sup>\*#</sup>**

<sup>\*</sup>Institute of Minerals and Materials Technology  
(Council of Scientific and Industrial Research)  
Bhubaneswar 751 013, India

<sup>\*\*</sup>Department of Mineral Science and Geophysics,  
Cochin University of Science and Technology, Cochin-682016, India

*(Received 10 October 2011; Accepted 7 December 2011)*

---

**Abstract**

*In this paper, an attempt is made to study the textural and grain size distribution, heavy mineral distribution pattern and chemical characteristics of fifteen red sediment samples collected from badlands to sea near Bhimunipatnam, Visakhapatnam Dist., Andhra Pradesh, India. The results of these studies indicate that the percentage of minerals' concentration of ilmenite, sillimanite, rutile and zircon are decreasing, whereas garnet is gradually increasing from badland to sea. The composite sample prepared from all fifteen samples contain 29.4 % Total Heavy Minerals (THM). The modal analysis of the THM indicates that the sample contains 48.3% ilmenite, 25.5% garnet, 20.2% sillimanite, 2.6% zircon, 2.4% rutile and 1.0% other minerals. The product obtained from this composite sample by using stage spirals contain 98.3% THM with 29.2% yield and 97.6% recovery which could be subjected to mineral separation plant to recover individual heavy mineral concentrates.*

**Key words:** *Textural, Heavy minerals, Red sediment, Badlands topography, Ilmenite, Zircon, Sillimanite, Spiral concentrator.*

---

**1. Introduction**

The red sediments of badlands topography are prominent features along the coastal belt of Bhimunipatnam Visakhapatnam Dist., Andhra Pradesh. These sediments are homogeneous, unfossiliferous and exhibit characteristic reddish colour, which gives the name red sediments. Because of their homogeneity

---

<sup>#</sup> *Corresponding author:* [bhimarao@immt.res.in](mailto:bhimarao@immt.res.in); [bhimarao@gmail.com](mailto:bhimarao@gmail.com)

and unconsolidated nature, they eroded and washed off continuously by the seasonal local streams. At places, these sediments characterized by the presence of calcium carbonate concretions exhibiting root like and stem like forms. These are consolidated and resistant to the drainage. They stand like pillars amidst the red sediment. The red sediments protected from erosion, where these concretions act like support structures. These sediments are mainly composed of mineral sand (including heavy placer minerals), silt and clay in which the mineral sand content nearly constitutes 90% of the total. The mineralogy of these sediments is almost similar to the nearby beach sands except the variation in individual mineral quantities. The mineral garnet is highly leached off along with other unstable minerals resulting iron oxide coating to all other mineral grains imparting red colour to these sediments. Hence, the presence of garnet is very less in this area. The red sand hills were once up to 40 metres high are now not more than 15 m. high and they extended from the Ramakrishna Beach area, Visakhapatnam to Bhimunipatnam [1, 2].

The red sediment deposit of Bhimunipatnam is having 10.55 km<sup>2</sup> area and an average elevation of 30 meters. There is no evidence of heavy mineral reserve estimation but these are large tonnage deposits. Deposits are being in badland, free from human settlement and easily accessible. Dominant kaolinite with subordinate illite is the general clay-mineral assemblage in both the red sediments and the soils. The similar clay-mineral composition indicates that the upland soils are the source for the clay

material in the red sediments. Montmorillonite is present in some samples and shows greater abundance in the red sediments than in the soils. The additional montmorillonite is considered to have been formed by post-depositional diagenesis in the red sediments at the expense of illite [3, 4].

Heavy minerals are located at the surface, hence mining is easy and no matter of over burden. Ilmenite is alone accounting to 60-65% in the deposit followed by sillimanite and zircon with little amount of monazite. Garnet is negligible in the badlands but also occurs in predominant in the stream deposits. Since these deposits are near to shore, there is no problem regarding environmental pollution or for deforestation. Setting up a mineral separation plant is justifiable as huge number unemployed fisher men are available for mining activities as well as for pre concentration of minerals at shore using sea water itself [5].

So far no attempt has been made either in India or elsewhere on placer heavy mineral concentration on recovery of total heavy minerals from the red sediments of badlands topography. In view of this, an attempt is made in this paper to assess the occurrence of placer heavy minerals, its characterization and its response to industrial gravity unit to recover total heavy minerals.

## 2. Location and study area

The location map of red sediment samples collected all along the fluvial plains of badlands topography of

Bhimunipatnam, Visakhapatnam Dist., Andhra Pradesh is shown in Fig 1.



**Figure 1.** The location map of red sediment samples are collected all along the fluvial plain of badlands topography of Bhimunipatnam, Visakhapatnam Dist., Andhra Pradesh

The study area Bhimunipatnam is located at 17.53N and 83.26E, about 20 km north of Visakhapatnam. It has an average elevation of 51 meters (170 feet). A predominantly red-looking sand deposit occurs extending over a 10.55 km<sup>2</sup> area up to 2.5 km inland from the beach road that runs along the backshore zone. The area is having a badland topography, which formed by the weathering and erosion, mainly by stream (rainwater run off) and wind action. Although the deposit is considered to be the product of several geomorphologic processes involving multiple cycles of deposition, a major part of it is considered as wind deposited dune sand except in its basal part Khondalites (garnet-sillimanite gneisses) are the predominant rock formations in the region in association with leptinites (garnet-biotite gneisses) and charnockites. Quartzite veins in khondalites and leptinites, besides sandstones and laterites also found as patches in the area.

### 3. Materials and methods

The typical morphological features of badlands topography of Bhimunipatnam, Andhra Pradesh is shown in Fig. 2 which clearly exhibit the concentration of heavies along the down stream flow of water towards beach. Fifteen number of red sediment surface samples (fifteen stream samples), containing heavy minerals were collected after rainy season from fluvial plain at an equal interval of 100 meters from the down hill to the sea.



**Figure 2.** Badlands topography of Bhimunipatnam, Visakhapatnam Dist., Andhra Pradesh

Initially, fifteen samples of each was scrubbed and deslimed separately by using hydrocyclone. Representative sub

samples were prepared from the individual deslimed sample using standard riffler sampler. Sub samples were studied for physical characterization, sink-float studies and mineralogical studies. Physical properties such as bulk density, true density and angle of repose along with size analyses of all the samples were carried out using standard sieves. The  $d_{80}$  percent passing size of each sample was calculated from the size analysis data. Each close size range of the sample was subjected to sink-float studies. Heavy liquid separation studies were carried out using bromoform (specific gravity 2.89  $\text{g/cm}^3$ ) for determining the total heavy minerals present in the feed samples.

Magnetic separation studies were carried out using dry high intensity magnetic separator using Permroll magnetic separator, developed by ELB-YANTV and supplied by Ore Sorters (Australia) Pty., Ltd. Mineralogical modal analysis was carried out using a Lecia petrological optical microscope. Powdered scrubbed product was subjected to X-ray diffraction (XRD) using PANalytical (X'pert) powder diffractometer, (scan speed-  $1.2^\circ/\text{min}$  from  $6^\circ$  to  $40^\circ$ , by Mo  $K\alpha$  radiation) to identify the mineral phases. Elemental analyses of the samples were carried out by XRF (PANalytical; PW2440 (MagiX PRO).

The fifteen samples were thoroughly mixed and prepared a composite sample for recovery of total heavy minerals from the feed using spiral concentrator. The deslimed composite sample was subjected to continuous stage spiral separation for recovery of total heavy minerals. Spiral studies were carried out using spiral concentrator having  $17 \frac{1}{2}$ " pitch,

manufactured by Humphrey's Mineral industries, Inc., USA with 30% solids concentration and the effect of wash water was also studied.

Operating conditions

Through put: 1200 kg/hr

Wash water: 3l/min

Pulp density: 30 % by weight

The concentrate and tailing fractions were collected, weighed, and then THM content was determined by sink-float method for analyzing the grade and recovery of the heavy minerals in the concentrate.

#### 4. Results and discussion

##### a) Textural and grain size distribution

Size frequency modes of all fifteen samples collected from fluvial plain are shown in Fig. 3. It is clearly seen from figure that the size frequency mode of 210  $\mu\text{m}$  is gradually increases from sample 1 to sample 8 and beyond that (sample 9 to sample 15) the frequency mode is slightly decreasing.

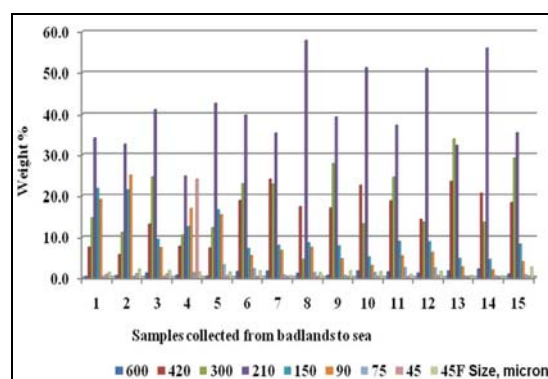
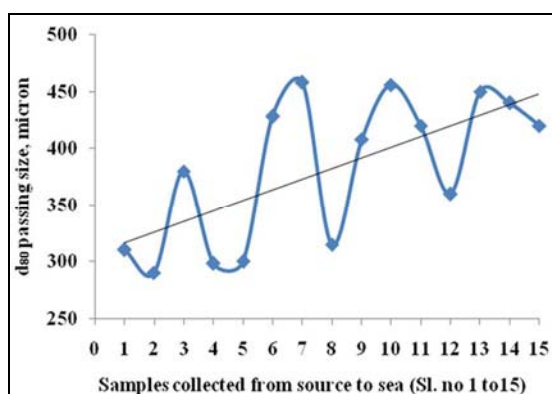


Figure 3. Size analysis of deslimed feed samples (Sl. no 1 to 15)

The particle size distribution characteristics from badlands to sea are shown in Fig. 4. It is clearly seen from the figure that the  $d_{80}$  passing size of the feed is gradually increases from source to sea. The  $d_{80}$  passing size of sample 1 is 310  $\mu\text{m}$  where as for sample 15 the  $d_{80}$  passing size is 420  $\mu\text{m}$ . It clearly indicates that towards sea the feed becomes coarser.



**Figure 4.** Particle size characteristics of deslimed feed samples

The  $d_{80}$  passing size of each fluvial sample is correlated with physical properties of the samples such as true density, bulk density, porosity and angle of repose which are given in Table 1.

The distribution patterns for true density of minerals present in fifteen samples are shown in Fig.5.

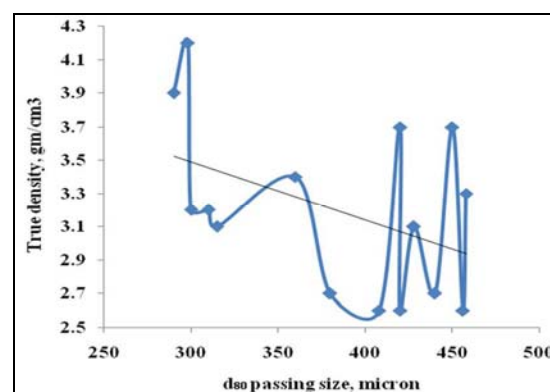


**Figure 5.** Distribution pattern of true density with respect to size of feed

**Table 1.** Physical properties of deslimed samples (Sl. No 1 to 15)

No. of sampling points	Bulk density, $\text{g/cm}^3$	True density, $\text{g/cm}^3$	Apparent porosity, %	Angle of repose, degree	$d_{80}$ passing size, $\mu\text{m}$	$d_{50}$ passing size, $\mu\text{m}$	$d_{10}$ passing size, $\mu\text{m}$
1	2.0	3.2	37.5	28.7	310	230	120
2	2.3	3.9	41.0	28.4	290	210	110
3	1.7	2.7	37.0	29.0	380	275	160
4	2.2	4.2	47.6	29.6	298	182	56
5	1.9	3.2	40.6	34.4	300	226	96
6	1.6	3.1	48.4	30.3	428	286	180
7	1.7	3.3	48.5	31.4	458	296	180
8	1.7	3.1	45.2	31.1	315	252	160
9	1.6	2.6	38.5	30.1	408	290	194
10	1.5	2.6	42.3	29.4	456	292	210
11	1.6	3.7	56.8	27.4	420	286	170
12	1.6	3.4	52.9	28.5	360	260	160
13	1.5	3.7	59.5	30.1	450	328	216
14	1.5	2.7	44.4	29.4	440	294	216
15	1.5	2.6	42.3	31.0	420	300	194

It can clearly be seen from the figure that with increase of particle size ( $d_{80}$  passing size 290  $\mu\text{m}$  to 458  $\mu\text{m}$ ) the true density of minerals is falling down. This observation can be expected as with increasing particle size, the total heavy mineral concentration decreases and the gangue minerals (quartz, feldspar etc.) whose specific gravity ( $2.6 \text{ g/cm}^3$ ) increases. Hence, the decrease in true density of the samples is justified.

As expected, the percentage of THM present in these samples shows a decreasing trend (Fig. 6) from a  $d_{80}$  passing size 290  $\mu\text{m}$  to 458  $\mu\text{m}$  (from badlands to sea).

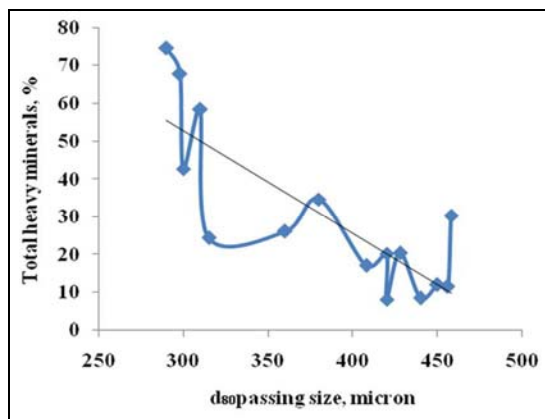


**Figure 6.** Distribution pattern of total heavy minerals with respect to size of feed

This observation is supported from sink float data that the THM are concentrated more in finer fractions. Fig. 7 shows the distribution pattern of total magnetic and non magnetic minerals in fifteen samples collected from badlands to sea. It is clearly seen from the figure that the percentage of magnetic minerals is gradually decreases towards sea where as the percentage of non magnetic minerals

are almost uniformly distributed from badlands to sea.

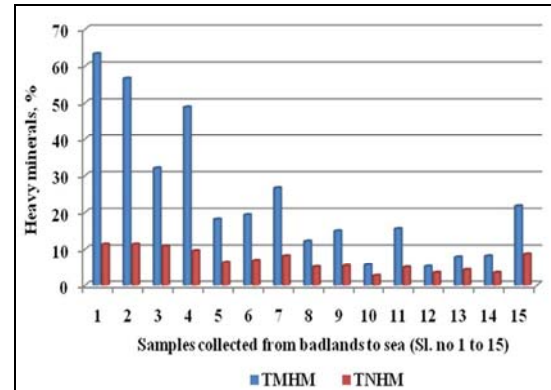


**Figure 7.** Distribution pattern of magnetic and non magnetic heavy minerals in deslimed feed samples

The size analysis magnetic heavy minerals present in samples, shown in Fig. 8 indicate that the percentage of magnetic minerals decreases gradually with decrease of  $d_{80}$  passing sizes of the samples from 458  $\mu\text{m}$  to 290  $\mu\text{m}$ .

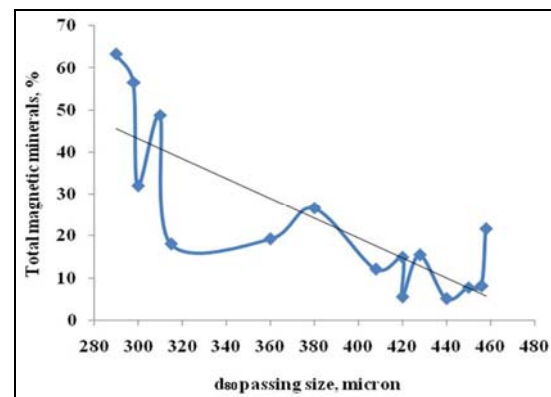


**Figure 8.** Distribution pattern of total magnetic minerals with respect to size of feed

Similar observation is also seen for total non magnetic heavy minerals present in fifteen samples collected from source to sea. It is clearly seen from Fig. 9 with

increase of particle size ( $d_{80}$  290  $\mu\text{m}$  to 458  $\mu\text{m}$ ) the percentage of non magnetic heavy minerals is falling down.

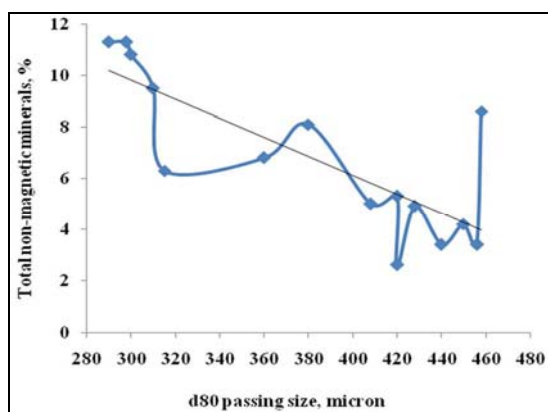


**Figure 9.** Distribution pattern of total non magnetic minerals with respect to size of feed

This observation indicates that the magnetic and non magnetic heavy

minerals are almost in the same size range.

### **b) Heavy minerals distribution pattern**

Results of sequential sink-float separation at 2.89 and 3.3 specific gravities on each sample collected from badlands to sea are given in Table 2 and their products are seen under microscope for mineralogical modal analysis.

The mineralogical modal analysis of heavy minerals of the study area is given in Table 3. The data are analyzed in terms of distribution pattern trend for individual heavy minerals in red sediment samples of different sampling points.

**Table 2.** Results of sink-float and high intensity magnetic separator on close sized fractions to recover magnetic and non-magnetics.

Samples collected	Deslimed feed			Magnetics			Non-magnetics		
	Sl. no	Wt., %	Sink,%	*THM	Wt., %	Sink,%	**TMHM	Wt., %	Sink,%
1	97.9	59.5	58.3	49.0	99.6	48.8	48.9	19.4	9.5
2	97.7	76.4	74.6	63.7	99.4	63.3	34.0	33.3	11.3
3	97.9	35.4	34.7	27.2	98.0	26.6	70.7	11.4	8.1
4	97.8	69.4	67.9	56.7	99.7	56.6	41.1	27.5	11.3
5	99.1	43.2	42.8	32.3	99.2	32.0	66.8	16.2	10.8
6	99.4	20.5	20.4	15.6	99.6	15.5	83.8	5.8	4.9
7	96.4	31.5	30.3	22.0	98.6	21.7	74.4	11.6	8.6
8	99.3	24.6	24.4	18.6	97.3	18.1	80.7	7.8	6.3
9	95.9	17.9	17.1	12.6	96.0	12.1	83.3	6.0	5.0
10	98.0	11.8	11.5	8.5	95.0	8.1	89.4	3.8	3.4
11	98.3	20.5	20.2	15.5	96.6	14.9	82.8	6.4	5.3
12	98.0	26.7	26.1	19.9	97.2	19.3	78.1	8.7	6.8
13	98.8	12.1	12.0	8.3	93.3	7.8	90.5	4.7	4.2
14	99.2	8.6	8.5	5.5	92.9	5.1	93.7	3.6	3.4
15	97.2	8.3	8.1	6.2	89.5	5.5	91.0	2.8	2.6

\*Total Heavy Minerals \*\*Total Magnetic Heavy Minerals \*\*\*Total Non-magnetic Heavy Minerals

**Table 3.** Distribution of placer heavy minerals in different locations of the study area (average)

No. of sampling points	Ilmenite, %	Garnet, %	Sillimanite, %	Rutile, %	Zircon, %	Others, %
1	72.9	10.8	8.7	3.4	3.6	0.5
2	73.5	11.4	6.4	3.6	4.7	0.4
3	58.2	18.4	16.7	2.9	3.2	0.6
4	54.3	29.0	8.5	3.8	4.1	0.1
5	46.5	28.3	17.5	4.2	3.3	0.2
6	41.2	34.8	19.1	2.0	2.5	0.5
7	40.3	31.4	20.5	3.6	3.0	1.3
8	43.0	31.1	19.7	2.9	2.0	1.2
9	39.8	31.0	22.8	2.3	2.9	1.2
10	34.8	35.7	23.5	0.9	0.9	4.3
11	42.1	31.7	20.8	3.0	2.0	0.5
12	42.5	31.4	20.3	2.7	2.3	0.8
13	29.2	35.8	30.8	0.8	1.7	1.7
14	28.1	31.7	35.2	0.4	1.2	3.5
15	32.1	35.8	29.6	0.4	1.2	3.7

Distribution pattern trend of ilmenite in fifteen samples is shown in Fig. 10.

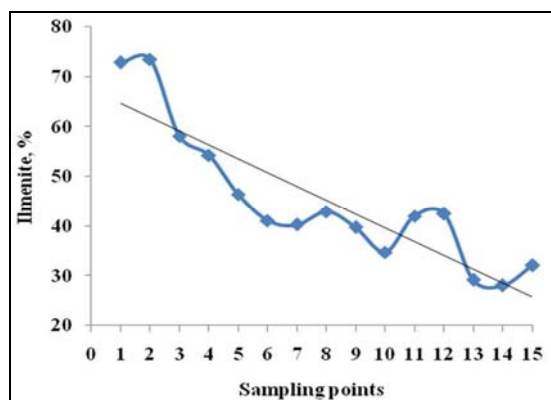


**Figure 10.** Distribution pattern trend of ilmenite in red sediment samples collected from badlands to sea (Sl. no 1 to 15)

It is seen that the ilmenite concentration is decreasing from badlands to sea. The decrease in ilmenite mineral concentration trend is more significant towards sea. The distribution pattern trend

of garnet present in samples is shown in Fig. 11; indicate that the garnet concentration is increasing from source to sea.

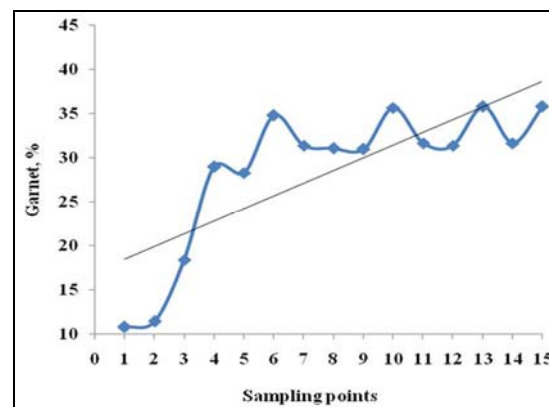


**Figure 11.** Distribution pattern trend of garnet in red sediment from badlands to sea (Sl. no 1 to 15)

The garnet mineral concentration trend is more significant towards sea. The correlation of ilmenite with respect to garnet is shown in Fig. 12. It is clearly

seen from the figure that the percentage of garnet is gradually decreasing with increase in the percentage of ilmenite or vice versa.

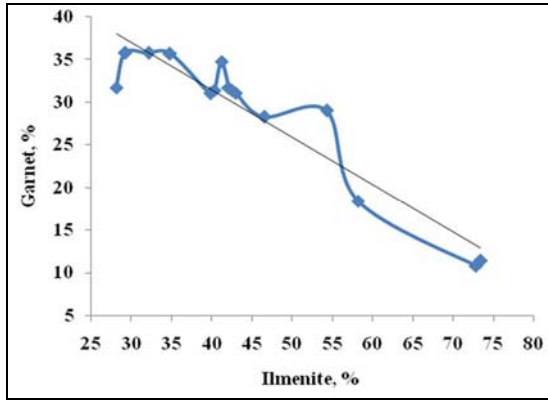


**Figure 12.** Correlation of garnet with ilmenite for samples collected from badlands to sea

The concentration of sillimanite in fifteen samples from source to sea has shown diverse nature from ilmenite. It is observed that the trend of sillimanite mineral concentration is increasing toward sea which can clearly be seen from Fig. 13.

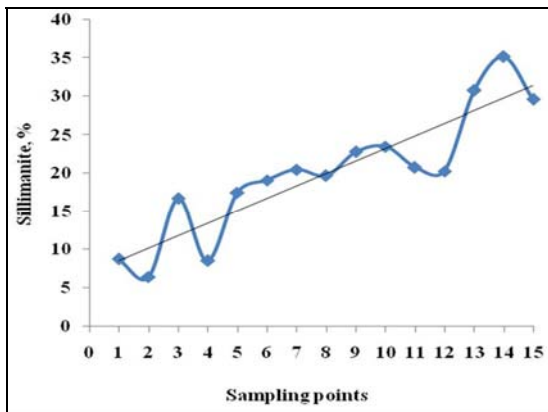


**Figure 13.** Distribution pattern trend of sillimanite in red sediment samples collected from badlands to sea (Sl. no 1 to 15)

The distribution pattern trend for rutile mineral concentration in fifteen samples shown in Fig. 14 indicates that rutile mineral concentration decreases from badlands to sea.

Similarly, the zircon mineral concentration shown in Fig. 15, indicate that the zircon mineral concentration also decreases gradually towards sea.

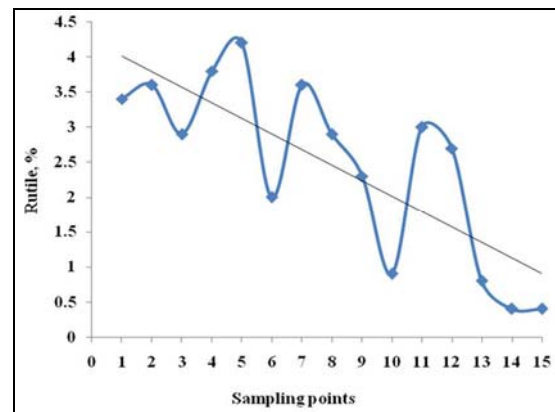


**Figure 14.** Distribution pattern trend of rutile in red sediment samples collected from badlands to sea (Sl. no 1 to 15)

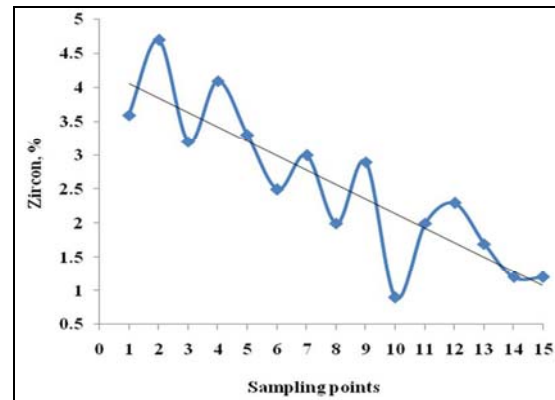


**Figure 15.** Distribution pattern trend of zircon in red sediment samples collected from badlands to sea (Sl. no 1 to 15)

The correlation of rutile with respect to zircon is shown in Fig. 16. It is clearly seen from the figure that the percentage of zircon is gradually increasing with increase in the percentage of rutile for samples towards sea.

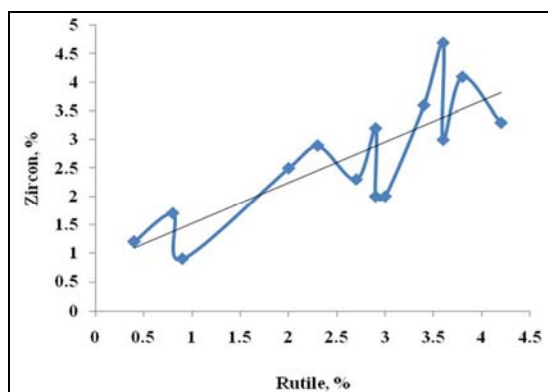


**Figure 16.** Correlation of zircon with rutile for samples collected from badlands to sea

However, it is concluded from the distribution pattern of all heavy minerals shown in Fig 17 that the trend of ilmenite, rutile and zircon minerals' concentration is decreasing from badlands to sea where as the trend for garnet and sillimanite mineral concentration is gradually increasing for samples collected from badlands to sea.

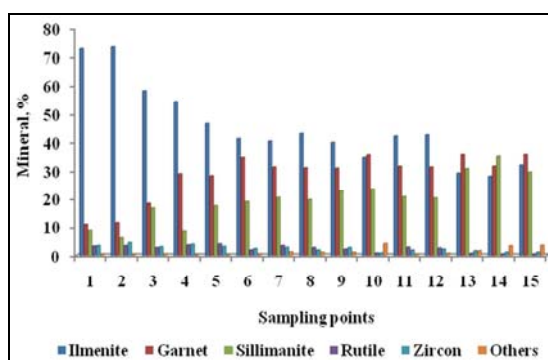


**Figure 17.** Distribution pattern of heavy minerals in deslimed feed samples collected from badlands to sea (Sl. no 1 to 15)

### c) Chemical characteristics

Chemical analysis of the magnetic heavy minerals and non magnetic heavy minerals of fifteen samples collected from badlands to sea are given Table 4.

The results of chemical analysis are correlated with reference to particle size distribution ( $d_{80}$  passing size,  $\mu\text{m}$ ) and possible mineral concentration. The data are presented in Figs. 18 to 24.

The distribution of  $\text{TiO}_2$  and  $\text{ZrO}_2$  content with reference to  $d_{80}$  passing sizes of red sediment samples are seen from Figs. 18 and 19.

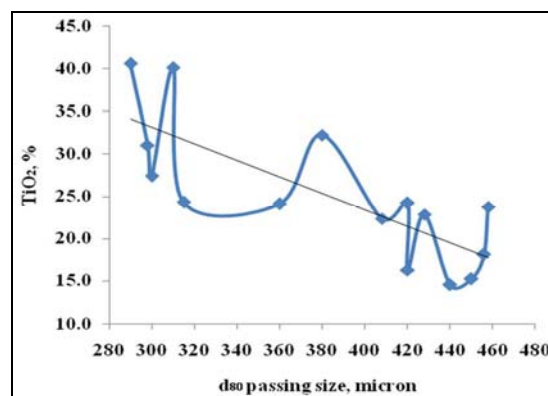


**Figure 18.** Distribution pattern of  $\text{TiO}_2$  in red sediment samples with respect to size feed

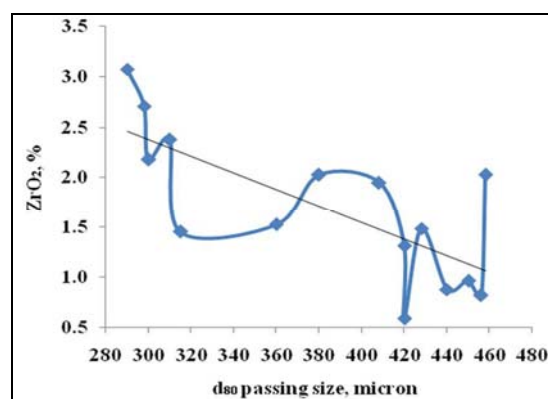


**Figure 19.** Distribution pattern of  $\text{ZrO}_2$  in red sediment samples with respects to size of feed

**Table 4.** Typical chemical analysis of sequential sink-float products of fluvial samples

Locations	Products	Wt, %	TiO <sub>2</sub> %	Fe <sub>2</sub> O <sub>3</sub> %	Al <sub>2</sub> O <sub>3</sub> %	SiO <sub>2</sub> %	MgO %	ZrO <sub>2</sub> %	HfO <sub>2</sub> %
1	Magnetic heavy minerals	48.8	43.991	48.490	3.969	3.204	0.233	0.112	0.001
	Non-magnetic heavy minerals	9.5	19.767	6.779	30.320	27.746	0.069	14.009	1.330
	Total	58.3	40.044	41.693	8.263	7.203	0.206	2.377	0.218
2	Magnetic heavy minerals	63.3	43.758	47.670	4.370	3.896	0.231	0.060	0.015
	Non-magnetic heavy minerals	11.3	22.468	5.298	24.157	26.472	0.048	19.949	1.608
	Total	74.6	40.533	41.252	7.367	7.316	0.203	3.073	0.256
3	Magnetic heavy minerals	26.6	38.425	49.582	6.560	5.127	0.245	0.031	0.031
	Non-magnetic heavy minerals	8.1	11.885	12.822	40.610	25.261	0.108	8.593	0.730
	Total	34.7	32.230	41.001	14.508	9.827	0.213	2.030	0.194
4	Magnetic heavy minerals	56.6	32.904	57.099	5.175	4.455	0.275	0.084	0.007
	Non-magnetic heavy minerals	11.3	21.504	6.385	29.110	26.173	0.054	15.835	0.950
	Total	67.9	31.007	48.659	9.158	8.069	0.238	2.705	0.164
5	Magnetic heavy minerals	32.0	31.432	57.058	6.198	4.994	0.284	0.012	0.022
	Non-magnetic heavy minerals	10.8	15.485	14.935	39.120	21.195	0.109	8.598	0.558
	Total	42.8	27.408	46.429	14.505	9.082	0.240	2.179	0.157
6	Magnetic heavy minerals	15.5	27.393	58.149	7.945	6.204	0.284	0.000	0.026
	Non-magnetic heavy minerals	4.9	8.507	13.459	44.620	26.644	0.112	6.184	0.494
	Total	20.4	22.857	47.415	16.754	11.114	0.243	1.485	0.138
7	Magnetic heavy minerals	21.7	28.464	58.876	6.832	5.520	0.284	0.012	0.035
	Non-magnetic heavy minerals	8.6	11.800	15.883	40.765	23.752	0.124	7.109	0.568
	Total	30.3	23.734	46.673	16.463	10.695	0.239	2.026	0.186
8	Magnetic heavy minerals	18.1	29.206	58.066	6.748	5.676	0.284	0.000	0.019
	Non-magnetic heavy minerals	6.3	10.105	12.803	43.491	27.221	0.103	5.627	0.649
	Total	24.4	24.274	46.379	16.235	11.239	0.237	1.453	0.182
9	Magnetic heavy minerals	12.1	28.412	58.174	7.198	5.886	0.295	0.012	0.024
	Non-magnetic heavy minerals	5.0	7.708	14.094	44.432	26.518	0.112	6.640	0.497
	Total	17.1	22.358	45.285	18.085	11.919	0.241	1.950	0.162
10	Magnetic heavy minerals	8.1	24.998	58.267	9.042	7.465	0.295	0.012	0.055
	Non-magnetic heavy minerals	3.4	1.671	11.888	45.542	37.705	0.117	2.737	0.340
	Total	11.5	18.101	44.555	19.833	16.406	0.242	0.818	0.139
11	Magnetic heavy minerals	14.9	28.963	57.376	7.309	6.067	0.284	0.012	0.011
	Non-magnetic heavy minerals	5.3	10.895	13.931	44.810	24.822	0.114	4.972	0.465
	Total	20.2	24.222	45.977	17.148	10.988	0.239	1.313	0.130
12	Magnetic heavy minerals	19.3	28.968	57.185	7.171	6.374	0.283	0.024	0.005
	Non-magnetic heavy minerals	6.8	10.259	12.509	44.210	26.612	0.110	5.788	0.521
	Total	26.1	24.094	45.545	16.821	11.647	0.238	1.526	0.139
13	Magnetic heavy minerals	7.8	22.608	57.490	10.495	9.169	0.293	0.000	0.055
	Non-magnetic heavy minerals	4.2	1.537	12.142	50.520	32.603	0.118	2.750	0.349
	Total	12.0	15.233	41.618	24.504	17.371	0.232	0.963	0.158
14	Magnetic heavy minerals	5.1	23.593	57.690	9.831	8.644	0.293	0.012	0.039
	Non-magnetic heavy minerals	3.4	0.863	15.051	49.918	31.548	0.150	2.172	0.297
	Total	8.5	14.501	40.634	25.866	17.806	0.236	0.876	0.142
15	Magnetic heavy minerals	5.5	23.460	56.965	10.452	8.853	0.294	0.012	0.038
	Non-magnetic heavy minerals	2.6	1.119	8.513	52.220	35.966	0.098	1.794	0.311
	Total	8.1	16.289	41.413	23.859	17.556	0.231	0.584	0.126

It is interesting to note from Fig. 18 that the percentage of TiO<sub>2</sub> content decreases with increasing d<sub>80</sub> passing size

for samples collected from source to sea. Similarly, ZrO<sub>2</sub> content decreases with

increasing  $d_{80}$  passing size for samples (Fig. 19).

The correlation between  $TiO_2$  and  $Fe_2O_3$  in the magnetic heavy minerals (mostly garnet and ilmenite) is plotted in Fig. 20.

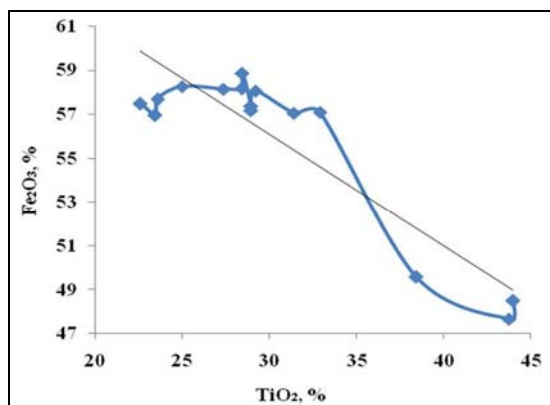


**Figure 20.** Correlation of  $Fe_2O_3$  with  $TiO_2$  for samples collected from badlands to sea

It is observed from  $TiO_2$  vs.  $Fe_2O_3$  (Fig. 20), with increase of  $Fe_2O_3$  the  $TiO_2$  content is decreasing in the magnetic heavy minerals (mostly garnet and ilmenite) of red sediment samples. This observation can be explained in two ways: i) as expected with decrease of  $Fe_2O_3$  content the  $TiO_2$  content increases as the process of alteration of mineral ilmenite,  $FeO \cdot TiO_2$  in nature involves the processes of oxidation and leaching whereby iron is progressively removed to give a residual product, essentially,  $TiO_2$  (Rutile) ii) ilmenite concentration is decreasing from source and garnet concentration is increasing towards to sea. The concentration of garnet is because of windblown sand from sea to inlands.

The correlation between the  $TiO_2$  content with  $Al_2O_3$  and  $ZrO_2$  plotted for non magnetic heavy minerals (mostly

sillimanite, rutile and zircon minerals) of fifteen samples collected from source to sea are shown in Figs. 21 and 22.

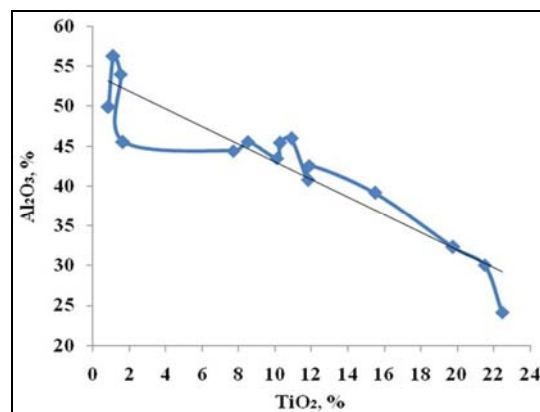


**Figure 21.** Correlation of  $Al_2O_3$  with  $TiO_2$  for samples collected from badlands to sea

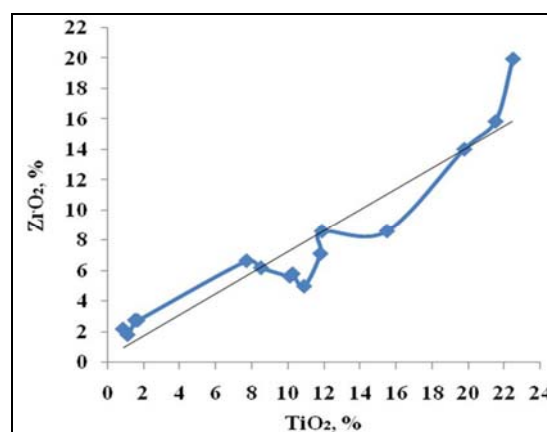


**Figure 22.** Correlation of  $ZrO_2$  with  $TiO_2$  for samples collected from badlands to sea

It is observed from Fig. 21 that the  $Al_2O_3$  content (mostly sillimanite mineral) decreases with increase of  $TiO_2$  content (mostly rutile mineral). The data seen from Fig. 22 that the  $ZrO_2$  content is gradually increasing with increase in  $TiO_2$  content. It indicates that the zircon mineral concentration increases with rutile concentration.

The correlation between the  $\text{Al}_2\text{O}_3$  content with  $\text{SiO}_2$  in non magnetic fraction is shown in Fig. 23. It is clearly seen from the figure that the  $\text{SiO}_2$  content is gradually increasing with increase in  $\text{Al}_2\text{O}_3$  content. Similarly,  $\text{HfO}_2$  content is increasing with increase in  $\text{ZrO}_2$  content in feed samples collected from badlands to sea (Fig. 24).

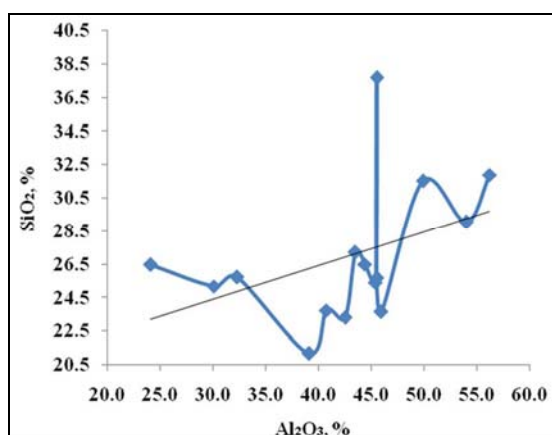


**Figure 23.** Correlation of  $\text{SiO}_2$  with  $\text{Al}_2\text{O}_3$  for samples collected from badlands to sea

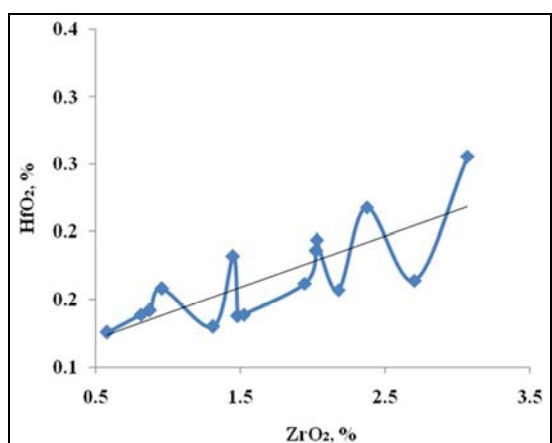


**Figure 24.** Correlation of  $\text{HfO}_2$  with  $\text{ZrO}_2$  for samples collected from badlands to sea

It is concluded from Figs. 18 to 24 that the correlation of  $\text{TiO}_2$  with  $\text{Fe}_2\text{O}_3$  in magnetic heavy minerals and  $\text{TiO}_2$  vs.

$\text{Al}_2\text{O}_3$  and  $\text{ZrO}_2$  in non magnetic heavy minerals that ilmenite concentration decreases from badlands to sea where as garnet concentration increases. It is also observed that sillimanite concentration is more significant than the rutile and zircon. Thus, the occurrence of minerals ilmenite, garnet, sillimanite, rutile and zircon are in order of abundance at this fluvial sampling area closer to sea.

These individual heavy minerals can be recovered after preconcentration of total heavy minerals by physical beneficiation methods for industrial applications.

#### **d) Beneficiation studies on composite sample to recover total heavy minerals**

Composite sample has been prepared by mixing all deslimed samples from Sl. no 1 to 15. The physical properties of composite sample are given in Table 5.

**Table 5.** Physical properties of composite sample

Details	Value
Bulk density, $\text{g/cm}^3$	1.7
True density, $\text{g/cm}^3$	3.2
Porosity, %	45.5
Angle of repose: degree	29.9
$d_{80}$ passing size, $\mu\text{m}$	310
Total Heavy Minerals (THM), %	29.4
Total Magnetic Heavy Minerals (TMM), %	22.8
Total Non -Magnetic Heavy Minerals (TNM), %	6.6
Very Heavy Minerals (VHM>3.3 Sp.Gr) , %	24.9
Light Heavy Minerals (LHM<3.3 Sp.Gr) , %	4.5
Slimes , %	4.1
Total iron (Fe, %) in slimes	8.1

The data indicate that the  $d_{80}$  passing size of the composite feed sample is 310  $\mu\text{m}$  and the total heavy mineral content is 29.4%. The average density of the sample is  $3.2 \text{ g/cm}^3$ . The modal analysis of the total heavy minerals of the composite sample shown in Fig. 25 indicate that the sample contain 48.3% ilmenite, 25.5% garnet, 20.2% sillimanite, 2.6% zircon, 2.4% rutile and 1.0% other minerals.

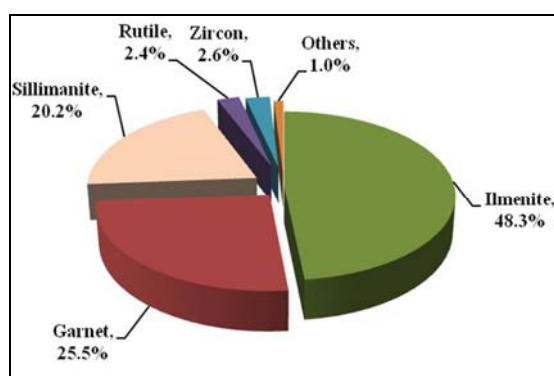


**Figure 25.** Model analysis of total heavy minerals of composite sample

X-ray diffraction pattern data of deslimed feed, magnetic heavies, non-magnetic heavies and slimes are given in Fig. 26.

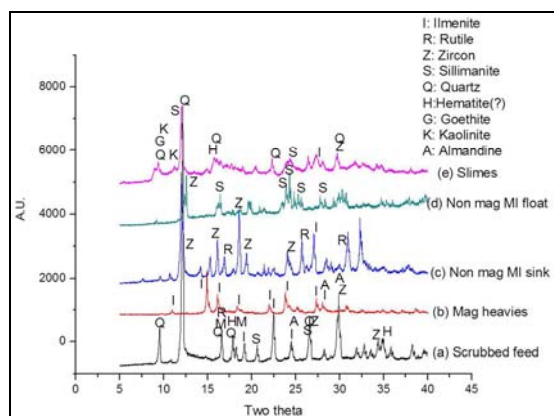


**Figure 26.** XRD pattern of deslimed feed, mag heavies, non mag MI sink, non mag MI float and slimes

The data indicate that the deslimed feed contains mostly quartz followed ilmenite and minor amounts of sillimanite, zircon, rutile, almandine, etc. (Fig. 26a). The magnetic heavies significantly exhibit the presence of ilmenite intensity peak (Fig. 26b), whereas the non magnetic very heavies significantly exhibit the presence of multiple mineral peak intensities such zircon, rutile etc (Fig. 26c). The non magnetic light heavy minerals exhibit the significant sillimanite peaks (Fig. 26d). The slimes contain largely quartz, kaolinite and associated with all probable heavy minerals in minor quantities (Fig. 26e).

The stereomicroscopic studies of magnetic heavies from THM are shown in Fig. 27 (a).

It is clearly seen from the figure that it contains maximum number of ilmenite (which is denoted with I) grains of varying forms such as rounded, sub rounded, elongated etc. The grains have pits and striations on that due to the grain to grain collision as well as collision with the obstacles in the path of transportation. Due to the high resistance of ilmenite most grains having sub-rounded (subhedral) or elongated nature.

A monazite (which is denoted with M) grain is also seen in the figure which is having a rounded form. The stereomicroscopic studies of non magnetic very heavy minerals from THM are given in Fig. 27(b). It reveals that it contains maximum number of rutile grains of elongated nature and zircon grains of euhedral form. Some of the rutile grains having iron coating and seen as opaque. Some pyriboles are also present of varying forms. The stereomicroscopic studies of

non magnetic light heavy minerals are shown in the Fig. 27(c), which gives the details that it mostly contains sillimanite grains of varying forms.

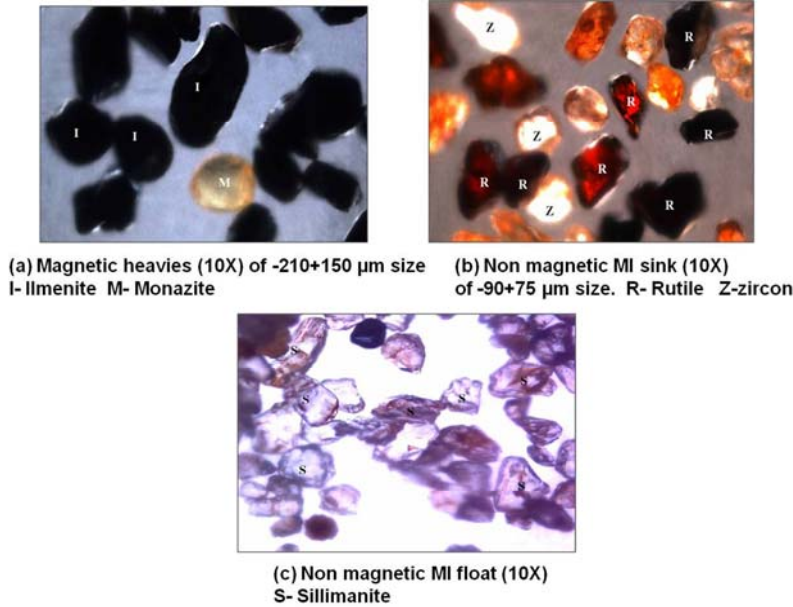


**Figure 27.** Stereomicroscopic photographs of magnetic heavies, non magnetic MI sink and non magnetic MI float of composite sample

A flow sheet is suggested with material balance on the recovery of total heavy minerals from red sediments of Bhimunipatnam, Visakhapatnam Dist., Andhra Pradesh. Minerals from stage spirals are shown in Fig. 28.

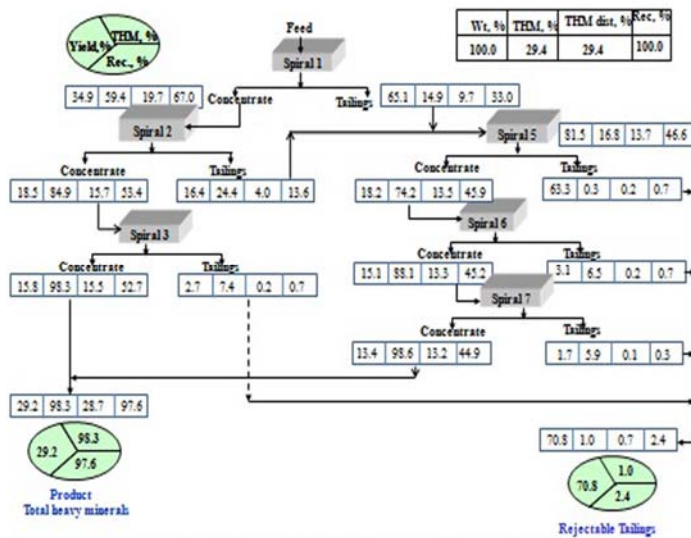


**Figure 28.** Flow sheet with material balance to recover total heavy minerals from red sediments of Bhimunipatnam, Visakhapatnam Dist., Andhra Pradesh

Summary of results on continuous spiral test for development of flow sheet with material balance are given in Table 6.

**Table 6.** Summary of stage spirals result on recovery of total heavy minerals

Details	Wt., %	Sink, %	THM, %	THM Rec, %
Concentrate (Product)	29.2	98.3	28.7	97.6
Tailings (Rejectable)	70.8	1.0	0.7	2.4
Total	100	29.4	29.4	100.0

The data indicate that the concentrate (Product-Total heavy minerals) contains 29.2% by weight with 98.3% THM and 97.6% recovery. The rejectable tailings contain 70.8% by weight with 1.0% THM loss.

## 5. Conclusions

The following conclusions are drawn based on the mineralogical, physical and chemical characteristics of all samples collected from badlands to sea (Sl. no 1 to 15) of Bhimunipatnam, Visakhapatnam Dist., Andhra Pradesh, India.

- The true density of minerals is falling down with increase of particle size ( $d_{80}$  passing size 290  $\mu\text{m}$  to 458  $\mu\text{m}$ ).
- The percentage of magnetic minerals is gradually decreasing towards sea where as the percentage of non magnetic minerals are almost uniformly distributed towards sea.
- The percentage of  $\text{TiO}_2$  and  $\text{ZrO}_2$  content decreases with increasing  $d_{80}$  passing size for samples collected from source to sea.

- Titaniferrous minerals such as ilmenite and rutile minerals concentration as well as zircon and sillimanite mineral concentration decreases from badlands to sea. However, garnet concentration is increasing towards sea
- With increase of  $\text{Fe}_2\text{O}_3$ , the  $\text{TiO}_2$  content is decreasing in the magnetic heavy minerals, while  $\text{Al}_2\text{O}_3$  content increases and the  $\text{TiO}_2$  content decreases for non magnetic heavy minerals.
- This red sediment deposit contains economic industrial minerals such as ilmenite, garnet, sillimanite, rutile and zircon in order of abundance.
- The end product obtained by using stage spirals contain 98.3% THM with 29.2% yield and 97.6% recovery which could be subjected to mineral separation plant to recover individual heavy mineral concentrates.
- Thus, it is concluded that the red sediments are potential resources for industrial placer minerals and can be recovered at first instance all total heavy minerals using spiral concentrator. Individual heavy minerals can be recovered from total heavy minerals concentrate for industrial applications.

## 6. Acknowledgements

The authors are thankful to the Prof. B.K. Mishra, Director, Institute of Minerals and Materials Technology (CSIR), Bhubaneswar for giving permission to publish this paper. Thanks also due to Mr. P.S.R Reddy, Head of Mineral Processing Department for his constant encouragement to carry out this work for

publication. One of the authors Ms. T. Laxmi is thankful to BRNS for granting SRF.

## **7. References**

- [1] Jagannadha Rao, M., Syam Kumar, J., Surya Prakasa Rao, B., Srinivasa Rao, P., Geomorphology and land use pattern of Visakhapatnam urban - Industrial Area, *Journal of the Indian Society of Remote Sensing*, Vol. 31, No. 2, (2003), pp. 119-128.
- [2] Nageswara Rao, K., Udaya Bhaskara Rao, Ch., Venkateswara Rao, T., Estimation of sediment volume through Geophysical and GIS analyses – A case study of the red sand deposit along Visakhapatnam Coast, *Journal of Indian Geophysics Union*, Vol.12, No. 1, (2008), pp. 23-30.
- [3] Durgaprasada Rao, N.V.N., Sriharia, Y., Behairy, A.K.A., Columnar concretions in the Visakhapatnam red sediments on the east coast of India, *Vol. 31, Issues 3-4*, (1982), pp. 303-316.
- [4] Durgaprasada Rao, N.V.N., Sriharia, Y., Clay mineralogy of the late pleistocene red sediments of the Visakhapatnam region, east coast of India, *Vol. 27, Issue 3*, (1980), pp. 213-215, 218-227.
- [5] Rao, J.M., Krishna Rao, J.S.R., Textural and mineralogical studies on red sediments of Visakhapatnam-Bhimunipatnam coast, *Geoviews*, Vol. 12, No. 2, (1984), pp. 57-64.